LAUTECH Journal of Computing and Informatics (LAUJCI) – ISBN : 2714-4194
Volume 5 No.1, April 2026 – www.laujci.lautech.edu.ng

An Intelligent Dermoscopic Image Analysis Framework for Skin Cancer Detection Using Enhanced Metaheuristic-Optimised Support Vector Machines

Olusola Bamidele Ayoade (Phd)
Emmanuel Alayande University of Education, Oyo
Department of Data Science, Informatics & Computer Science
ayoadeob@eauedoyo.edu.ng

Mumini Oyetunji Raji (Phd)
Emmanuel Alayande University of Education, Oyo
Department of Data Science, Informatics & Computer Science
rajimo@eauedoyo.edu.ng

Aminat Adejoke Akindele
Emmanuel Alayande University of Education, Oyo
Department of Data Science, Informatics & Computer Science
akindeleaa@eauedoyo.edu.ng

Kemi Jemilat Yusuf-Mashopa
Emmanuel Alayande University of Education, Oyo
Department of Data Science, Informatics & Computer Science

Muinat Folake Abdulrauff
Emmanuel Alayande University of Education, Oyo
Department of Data Science, Informatics & Computer Science

Ibrahim Adebayo Raji
Emmanuel Alayande University of Education, Oyo
Department of Data Science, Informatics & Computer Science
rajiia@eauedoyo.edu.ng

Fatima Bolanle Musah
Emmanuel Alayande University of Education, Oyo
Department of Data Science, Informatics & Computer Science
yusuf-mashopa@eauedoyo.edu.ng

Olufemi Micheal Amuda
Emmanuel Alayande University of Education, Oyo
Department of Data Science, Informatic & Computer Science
abdulrauffmf@eauedoyo.edu.ng

ABSTRACT

Skin cancer is among the most common and lethal malignancies globally, with its high mortality rate primarily due to delayed diagnosis and insufficient early detection. Despite recent advancements, current computer-aided diagnostic techniques frequently exhibit restricted classification accuracy, high computational complexity, and ineffective hyperparameter optimisation, thereby limiting their efficacy in practical clinical settings. This study aims to create efficient and robust intelligent models for precise skin cancer detection and classification by improving optimisation-driven machine learning techniques. The study proposes two enhanced multi-class Support Vector Machine (SVM)-based frameworks to achieve this objective: MCMLMBSVM-EAO and MCMLMBSVM-EHHO. The study aims to: (i) improve dermoscopic image quality via preprocessing techniques such as resizing, grayscale conversion, contrast enhancement, and noise reduction; (ii) accurately segment lesion regions using the Sobel edge detection method; (iii) extract discriminative colour, shape, and texture features using Colour Moments and Gray Level Co-occurrence Matrix (GLCM); and (iv) enhance SVM classification efficacy through sophisticated hyperparameter optimisation. To address intrinsic optimisation challenges, the Aquila Optimiser (AO) and Harris Hawks Optimiser (HHO) are methodically refined with innovative mechanisms to augment convergence speed, search efficacy, and solution robustness. The proposed models are assessed using the benchmark HAM10000 dermoscopic dataset. Experimental findings indicate that the MCMLMBSVM-EAO and MCMLMBSVM-EHHO models attain classification accuracies of 98.45% and 98.67%, respectively, surpassing

numerous leading methodologies. The findings underscore the efficacy, resilience, and generalisability of the proposed frameworks, rendering them appropriate for dependable and efficient automated dermatological diagnosis, especially in resource-limited settings.

Keywords: Automated diagnosis, Dermoscopic image analysis, Hyperparameter optimisation, Medical image classification, Skin cancer detection

1. INTRODUCTION

Skin cancer has become a swiftly increasing global public health issue, with potentially lethal consequences if diagnosis is delayed. The development of skin cancer can be attributed to various risk factors, such as prolonged exposure to ultraviolet (UV) radiation, environmental factors, lifestyle decisions, viral infections, allergic reactions, and other biological or physical conditions. Excessive UV exposure has been recognised as a significant contributing factor, as it can cause DNA damage in skin cells and initiate abnormal cellular proliferation, potentially resulting in malignant transformation [1]. Atypical tissue proliferation and persistent skin lesions are frequently considered early signs of potential malignancy in clinical practice. Skin cancer is primarily divided into several types, including actinic keratosis, basal cell carcinoma, squamous cell carcinoma, and melanoma. Epidemiological research in Southwestern Nigeria reveals that squamous cell carcinoma is the most prevalent histological subtype of skin cancers in the area [3]. Nigeria reports roughly 65,258 new skin cancer cases each year, with an incidence rate of approximately 52 per 100,000 individuals, rendering it one of the most frequently diagnosed cancers in the nation [4].

Conventional diagnostic techniques for skin cancer, such as visual assessment and histopathological biopsy, continue to be the clinical gold standard. Nonetheless, these methods are frequently invasive, time-intensive, and heavily reliant on clinician proficiency, potentially leading to diagnostic inconsistency and an increased risk of human error [5]. Dermatologists who depend exclusively on dermoscopic images may face constraints in diagnostic precision, especially when evaluating early-stage lesions with nuanced visual characteristics [6]. In numerous instances, conclusive verification still necessitates biopsy examination, potentially prolonging both diagnosis and treatment, thus underscoring the demand for more effective and dependable diagnostic methods. Therefore, the creation of automated and reliable systems for the early detection and precise classification of skin cancer is crucial to improve treatment outcomes and increase patient survival rates [7].

In addressing these challenges, numerous studies have investigated the application of machine learning techniques for the automated detection and classification of skin cancer, particularly focusing on support vector machine (SVM)-based methodologies. The authors in [8] created an intelligent diagnostic framework that incorporates image preprocessing, segmentation, and feature extraction methods. Their methodology utilised morphological operations, including black-Hat transformation and inpainting, for digital hair removal, while Gaussian filtering was implemented for noise reduction. Lesion regions were defined utilising the GrabCut algorithm, and distinctive texture and statistical features were obtained through the Gray Level Co-occurrence Matrix (GLCM). The extracted features were classified using decision tree, K-nearest neighbour, and SVM classifiers on the ISIC-2019 and HAM10000 datasets, with the SVM classifier exhibiting significantly superior performance.

The authors in [9] proposed an automated diagnostic system for detecting various

dermatological conditions, including acne, cherry angioma, melanoma, and psoriasis. Their framework utilised a multi-stage pipeline that included image acquisition, preprocessing, segmentation, feature extraction, and classification. The experimental assessment utilising Support Vector Machine (SVM), Random Forest (RF), and K-Nearest Neighbour (KNN) classifiers produced classification accuracies of 90.7%, 84.2%, and 67.1%, respectively. The results demonstrated that the SVM-based model attained the highest overall performance, despite some related studies reporting slightly superior accuracies. The authors in [10] proposed an evolutionary machine learning framework for skin disease detection that integrates preprocessing, augmentation, segmentation, and classification techniques. Experimental findings indicated that the SVM classifier reached a maximum accuracy of 98.8%, whereas KNN achieved a sensitivity of 91% and a specificity of 99%, thereby underscoring the efficacy of machine learning methodologies in dermatological image analysis. Recently, the authors in [11] created a machine learning system for the detection and classification of different types of skin cancer utilising dermoscopic images. Their methodology utilised SVM classifiers trained on colour, texture, and shape features to differentiate malignant from benign lesions, attaining an accuracy of approximately 97%.

Nonetheless, while existing studies on skin disease detection have shown the efficacy of machine learning models, especially Support Vector Machines (SVMs), in classifying dermoscopic images, numerous significant constraints remain unaddressed. A significant deficiency in previous studies is the absence of sophisticated and adaptive hyperparameter optimisation strategies. Numerous studies depend on traditional or static tuning methods that limit the optimal performance of SVM in intricate, high-dimensional search spaces. Insufficient parameter tuning may result in overfitting, slow convergence, and suboptimal generalisation performances, especially in medical image classification tasks defined by nonlinear and high-dimensional feature spaces [12–13]. Furthermore, existing optimisation approaches frequently demonstrate an imbalance between exploration and exploitation, leading to premature convergence, inadequate local search efficacy, and diminished population diversity. Moreover, numerous prior frameworks exhibit restricted robustness and generalisation ability due to insufficient management of class imbalance, overfitting, and the intrinsic variability of dermoscopic images. A significant limitation exists in inadequate feature representation, wherein colour, texture, and shape features are either insufficiently incorporated or not efficiently optimised for discriminative learning. Moreover, certain methodologies exhibit increased computational complexity or inefficiency, especially those reliant on deep learning models, thus constraining their applicability in resource-limited settings. In our previous studies, non-hybrid optimisation- based learning models were established, utilising the Aquila Optimiser (AO) and Harris Hawks Optimiser (HHO) independently to optimise SVM hyperparameters for the detection and classification of skin diseases. The Aquila Optimiser exhibits robust global exploration capabilities; however, its efficacy may be compromised by premature convergence and insufficient local exploitation in intricate SVM search spaces [14]. The Harris Hawks Optimiser demonstrates proficient exploitation behaviour; however, it may experience constrained exploration and diminished population diversity, potentially impairing optimisation performance in multimodal and high-dimensional search challenges, such as SVM parameter tuning [15–16].

Despite recent advancements, current computer-aided diagnostic techniques frequently exhibit restricted classification accuracy, high computational complexity, and ineffective

hyperparameter optimisation, thereby limiting their efficacy in practical clinical settings.To address these limitations, this study introduces two sophisticated optimisation-driven frameworks, EAO-MCMLMBSVM and EHHO-MCMLMBSVM, which significantly improve SVM-based classification of skin diseases. The study presents enhanced versions of the Aquila Optimiser (AO) and Harris Hawks Optimiser (HHO) through the integration of various innovative mechanisms. The improved AO incorporates a Search Control Factor (SCF), adapted from [17] to dynamically balance the global exploration and local exploitation throughout various stages of the optimisation process. Furthermore, Fast Random Opposition-Based Learning (FROBLAO), adapted from [18], is used to enhance population diversity and expedite convergence by simultaneously assessing candidate solutions and their respective opposite positions within the search space. Additionally, Gaussian Mutation (GM), adapted from [17], is used to enhance local search in proximity to high-quality candidate solutions, facilitating a more accurate adjustment of essential SVM hyperparameters, namely C and γ. These enhancements collectively enhance convergence speed, optimisation robustness, and classification performance within the proposed EAO-MCMLMBSVM framework. The Harris Hawks Optimiser is improved by incorporating a Double Adaptive Weights Strategy, adapted from [19], which dynamically modifies exploration and exploitation processes to attain more stable convergence to optimal SVM parameters. The Dimension Learning-Based Hunting (DLH) mechanism, adapted from [20–21], is implemented to enable cross-dimensional knowledge transfer among candidate solutions, thus enhancing the search coverage within the hyperparameter space. Additionally, a position update strategy adapted from the Dung Beetle Optimiser (DBO), as suggested in [22], is used to improve local search efficacy while preserving population diversity, which is crucial for preventing premature convergence and facilitating thorough exploration of the solution space. These modifications enhance convergence accuracy, stability, and generalisation capacity within the proposed EHHO-MCMLMBSVM framework.

The classification of skin diseases presents a formidable challenge owing to pronounced intra-class similarity, considerable inter-class variability, and the nonlinear attributes of dermoscopic images [6, 23-24]. Integrating these enhancement strategies into AO and HHO before SVM hyperparameter optimisation enables the proposed models, EAO-MCMLMBSVM and EHHO-MCMLMBSVM, to attain a superior balance between exploration and exploitation, enhanced convergence stability, and a more efficient hyperparameter search process. Additionally, a position update strategy adapted from the Dung Beetle Optimiser (DBO), as suggested in [22], is used to improve local search efficacy while preserving population diversity, which is crucial for preventing premature convergence and facilitating thorough exploration of the solution space. The main contributions of this study can be summarised as follows:

(i) This study proposes two advanced non-hybrid optimisation frameworks, EAO-MCMLMBSVM and EHHO-MCMLMBSVM, to overcome the performance limitations of Aquila Optimiser (AO) and Harris Hawks Optimiser (HHO). These frameworks significantly differ from previous studies that utilise only standalone optimisation methods. This research methodically improves the internal mechanisms of AO and HHO before applying them to Support Vector Machine (SVM) hyperparameter tuning, resulting in a more efficient and stable optimisation process.

(ii) The improved Aquila Optimiser integrates a Search Control Factor (SCF) to establish an adaptive balance between exploration and exploitation. It employs Fast Random Opposition-Based Learning (FROBLAO) to enhance population diversity

and expedite convergence. Gaussian Mutation (GM) enhances local search efficacy. The enhanced Harris Hawks Optimiser incorporates a Double Adaptive Weights Strategy, Dimension Learning-Based Hunting (DLH), and a position update mechanism inspired by the Dung Beetle Optimiser. These enhancements collectively address prevalent optimisation challenges, such as premature convergence, inadequate local exploitation, and limited search diversity, commonly noted in existing literature.

(iii) The study presents a comprehensive multi-feature extraction framework that incorporates colour moments, shape descriptors, and texture features derived from the Grey Level Cooccurrence Matrix (GLCM). This detailed feature representation accurately captures the intricate, nonlinear attributes of dermoscopic images, thereby improving class separability in scenarios characterised by significant intra-class similarity and inter-class variability. This issue continues to be inadequately addressed in numerous prior approaches.

(iv) A balanced dataset strategy is implemented by selecting equal samples from eight clinically significant skin disease categories within the DermNet dataset. This method directly addresses the prevalent issue of class imbalance, thereby enhancing generalisation performance and reducing classification bias.

2. METHODOLOGY

This section describes the materials, dataset sources, and methodologies employed in developing the two classification models proposed in this study, namely EAO-MCMLMBSVM and EHHO-MCMLMBSVM. As highlighted in the introduction, the primary objective of this research is to evaluate the effectiveness of enhanced machine learning models in addressing common limitations reported in previous studies, including class imbalance, high false positive rates, model overfitting, and excessive computational complexity. To rectify the problem of class imbalance, an equal quantity of samples was initially chosen for each disease category. Subsequently, two classification models were developed, and the data preparation process is thoroughly detailed, with a specific focus on the input data employed by both models. The proposed models were subsequently applied to extract informative features, minimise overfitting, and optimise the discriminative hyperparameters of the MCMLMBSVM classifier. These procedures enhance computational efficiency while minimising the occurrence of false positives. Figure 1 displays the block diagram depicting the comprehensive framework of the proposed methodology.

2.1 Image Acquisition

The proposed system was developed utilising dermatoscopic images sourced from the DermNet Skin Disease dataset, accessible via the Kaggle repository (https://www.kaggle.com/datasets/dedeikhsandwisaputra/skin-disease-dermnet). The dataset comprises images of 23 distinct skin disease categories; however, only eight categories were chosen for this study to guarantee balanced representation and optimal model training. A total of 2,700 dermatoscopic images were employed, with the same number of datasets chosen at random for each class of the diseased datasets to avoid having an uneven dataset for class labelling. The dataset is divided into nine categories: 700 photos showing normal skin, 250

photos each showing dermatofibroma (DEM), benign keratosis (BEK), actinic keratosis (ACK), melanoma (MEM), psoriasis (PSO), scabies (SCA), basal cell carcinoma (BCC), and eczema/atopic dermatitis (ECZ), respectively. The dataset was divided into training and testing with 90% and 10%, respectively, with k-fold cross-validation of 10. Therefore, 2,430 datasets were used for testing, and the remaining 270 datasets were used for training, as shown in Table 1.

2.2 Image Preprocessing

The skin images may contain unwanted hair, noise, or distortion; therefore, the skin images need to be processed to enable the classification model to achieve better performance. The preprocessing steps in this study include image resizing, hair removal, and noise removal.

2.2.1 Image Resizing

In this study, we resized all the input images to a size of 512 × 512 using MATLAB's image resizer toolbox to eliminate unnecessary pixel information and streamline the classification model to reduce processing time and improve the overall model's performance.

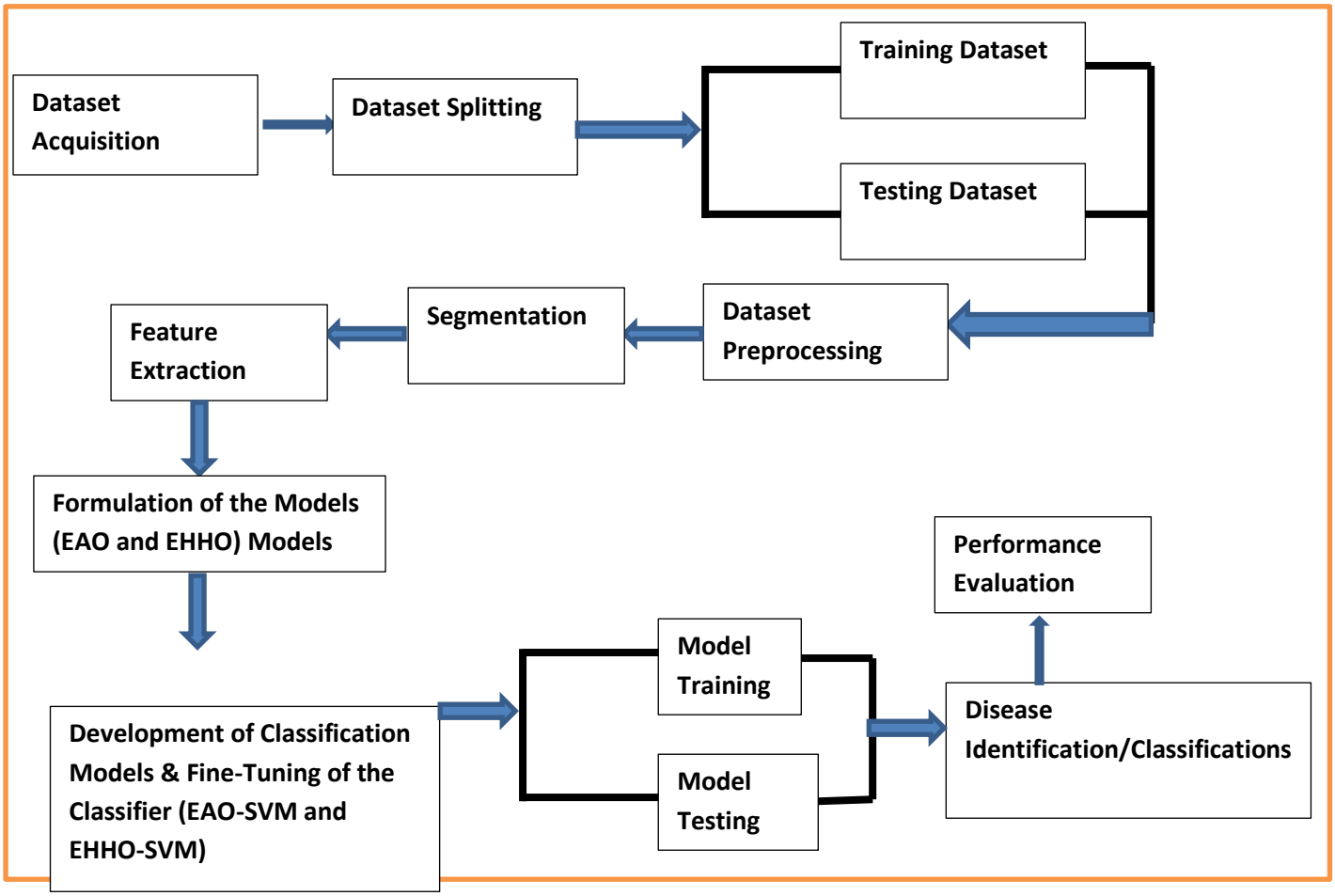

Figure 1. Proposed methodology block diagram

Table 1. Distribution of the cassava dataset acquired from the kaggle village

Class	Content	Number of Images per Class	Number of Training Datasets	Number of Testing Datasets
1	Dermatofibroma (DEM)	250	2,430	270
2	Benign Keratosis (BEK)	250		
3	Actinic Keratosis (ACK)	250		
4	Melanoma (MEM)	250		
5	Psoriasis (PSO)	250		
6	Scabies (SCA)	250		
7	Basal Cell Carcinoma (BCC)	250		
8	Eczema/Atopic Dermatitis (ECZ)	250		
9	Normal Skin	700		

2.2.2 Hair Removal

Researchers have employed several techniques, such as a median filter, adaptive threshold, and Gabor filtering, to remove hairs from skin images. This study used a digital hair removal (DHR) algorithm based on morphological filterings, such as Black-Hat transformation and the inpainting algorithm as described by the authors in [8], to remove hair in the images of skin. The steps of this DHR algorithm are given below:

1. Convert RGB images into grayscale images using the luminosity method, indicated by Equation 1, which was put forth by the authors in [26].
2. *Grayscale=0.2989 * Red + 0.587 * Green + 0.114 * Blue* (1)
3. Apply the Morphological Black-Hat transformation on the grayscale images
4. Create a mask for the inpainting task
5. Apply the inpainting algorithm on the original image using this mask.

2.2.3 Noise Removal

Image noise was mitigated through an adaptive median filtering technique to maintain essential structural details while attenuating extraneous noise.

2.3 Segmentation

The suggested models use the Sobel edge detection method to separate lesions from the uninfected part of the skin. The process of using the Sobel edge detection method involved two stages. Firstly, the gradient of the image along the x-axis and y-axis is determined using the Sobel operator. After finding the image gradient, the next step is to find a threshold value automatically so that edges can be determined. According to the Authors in [27], equations 2, 3, 4, and 5 were used to compute the image gradient along the x and y-axis and equations 6, 7 and 8 were used to

calculate the threshold value. Algorithm 1 demonstrated an example of the image-dependent threshold computation and edge point Algorithm's pseudo-code.

$$g_x = \frac{\delta f}{\delta x} = (z_7 + 2z_8 + z_9) - (z_1 + 2z_2 + z_3) \quad (2)$$

$$g_y = \frac{\delta f}{\delta y} = (z_3 + 2z_6 + z_9) - (z_1 + 2z_4 + z_7) \quad (3)$$

Then the gradient of the image is defined as:

$$\nabla f(x,y) = \frac{\delta f}{\delta x}\hat{h} + \frac{\delta f}{\delta y} = g_x\hat{h} + g_y\hat{s} \quad (4)$$

where f(x,y) is the image, g(x,y) is the gradient image and $\hat{h}$ & $\hat{s}$ are unit vectors along the *x* and *y* axes, respectively. The magnitude of the gradient is given by equation 3.5:

$$g(x,y) = |\nabla f(x,y)| = \sqrt{gx^2 + gy^2} \quad (5)$$

Algorithm 1: Computation of Threshold Value of the Image (Source: [27])

1: Input: a, height of the image, b, width of the image, and g(x,y): gradient of the image

2: Utilising Equation 3.6, compute the average intensity of the gradient image g(x,y)
The initial threshold, Thd^0, is equal to the average intensity of the gradient image *g(x, y)*, as defined in equation 3.6

$$Thd^0 = \frac{\sum_{k=1}^{a}\sum_{l=1}^{b} g(x,y)}{a \times b} \quad (6)$$

3: Set iteration index $i = 0$, separate *g(x,y)* into two classes, where the lower class consists of those pixels of *g(x,y)* which have gradient values less than Thd^i, and the upper class contains the rest of the pixels.

4: Compute the average gradient values m_{Low} and m_{High} of the lower and upper classes, respectively.

5: Set iteration $i = i+1$ and update threshold value as:

$$Thd^i = \frac{m_{Low} + m_{High}}{2} \quad (7)$$

6: Repeat steps 2 to 4 until $|Thd^i - Thd^{i-1}| \leq \epsilon$, where $\epsilon \rightarrow 0$ and take Thd^i as the final threshold and denote it by *Thd.*

7: Compute the output utilising equation 3.8

$$E(x,y) = \begin{cases} 255 & g(x,y) \geq Thd, \\ 0 & otherwise \end{cases} \quad (8)$$

8: Comparing the value of the gradient image with the threshold value to determine the output:
If g*(x,y)* > *Thd*
Output: Return edge point (represented as white)
Endif
If *g(x,y)* < *Thd*
Output: Return background point (represented as black)
Endif

2.4 Feature Extraction

Texture, shape, and colour features were extracted from the segmented images utilising the Gray Level Co-occurrence Matrix (GLCM) and colour moment descriptors. The GLCM is extensively utilised for texture analysis as it captures the spatial relationships among pixel intensities and offers statistical measures that characterise the inherent texture patterns of lesions. This study computed five texture features, energy, contrast, homogeneity, correlation, and entropy, from the GLCM to represent textural characteristics, according to the authors in [28], represented by equations 9-13. Furthermore, six morphological features, eccentricity, area, solidity, rectangularity, equivalent diameter, and perimeter, according to the authors in [29], represented by equations 14-21, were extracted to characterise the lesions' properties. To enhance the capture of colour information, four colour moment statistics, medium, standard deviation, asymmetry, and kurtosis, were computed, according to the authors in [30], represented by equations 22-25, offering a thorough representation of the colour distribution within the lesion areas. In this study, the angle Θ can be found at angles of 0, 45, 90, and 135 degrees, with the distance d set to 50. The extracted texture, shape and colour features and their description and formula are given in Table 2.

Table 2. Different types of extracted features in the study

Feature Name	Description	Formula
Energy	It yields the sum of squared elements in the GLCM with a value of 0 to 1.	$Energy(l,\eta)=\sum_{e=1}^{Mg}\sum_{f=1}^{Mg}Q(e,f,l,\eta)2$ (9)
Contrast	It is the overall intensity of a pixel's relationship with its neighbour.	$Contrast(l,\eta)=\sum_{e=1}^{Mg}\sum_{f=1}^{Mg}(r-s)2Q(e,f,l,\eta)$ (10)
Correlation	It returns a measure of how closely a pixel is connected to its neighbours throughout the entire image.	$Correlation(l,\eta)=\sum_{e=1}^{Mg}\sum_{f=1}^{Mg}(e-m_r)\times(f-m_r)\times Q\times(e,f,l,\eta)/\mu_r\times\mu_s$ (11)
Homogeneity	It is defined as the closeness rate of distributed elements in GLCM.	$Homogeneity(l,\eta)=\sum_{e=1}^{Mg}\sum_{f=1}^{Mg}1/1+\mid e-f\mid Q\times(e,f,l,\eta)$ (12)

Entropy	It is the degree of uniformity between pixels within the image and randomness.	$EntropyENT(l,\eta) = -\sum_{e}^{Mg}\sum_{f}^{Mg} Q\times(e,f,l,\eta)/k\times Q\times(e,f,l,\eta)$ (13)
Eccentricity	It is the ratio of the major to minor axes.	$ECC = 2\times\sqrt{\left\{\left(\frac{utmost\ axis}{2}\right)^2 - \left(\frac{trivial\ axis}{2}\right)^2\right\}}$ (14) where the trivial and utmost axes' lengths are located using $Utmost\ axis\ length = a_1 + \mu$ (15) *Trivial* axis length $\sqrt{(a_1+a_2)^2 - c}$ (16) where a_1 and a_2 are the separations in the image between the focus and the points in the image, and c indicates the distance between the foci.
Area	For each I * J picture or a section of the picture, the **area** can be seen in this way	$x = \sum_{d=1}^{I}\sum_{e=1}^{J} X[d,e]$ (17)
Solidity	The convex hull area divided by the spot area yields the **solidity** value. It shows whether a region is convex or concave in shape. A shape is fully compacted when its solidity value is 1.	$Solidity = \frac{X_i}{X_j}$ (18) where X_i represents the area of a lesion or spot shape, and X_j stands for the area of a lesion shape's convex hull.
Rectangularity	The term "**rectangularity (extent)**" refers to how rectangular a	Rectangularity $= \frac{X_i}{X_J}$ (19)

	spot's form is. If a spot receives a rectangularity rating of 1, it has an exact rectangular form.	where X_J is the smallest area covered by the bounding rectangle. The smallest rectangle that encompasses every point in the shape is known as the minimum bounding rectangle
Equidiameter	A disc that resembles a spot is measured by its **equidiameter**	Equidiameter $= \sqrt{\left\{\frac{4\times Spot\ Area}{3.142}\right\}}$ (20)
Perimeter	is a **shape (morphological) feature** used in image analysis to describe the **length of the boundary of an object**, such as a segmented skin lesion in a dermoscopic image	Perimeter = 2(len + wid) (21) where the length is denoted by len and the width by wid
Medium	η represents the average pixel intensity and describes the image's general brightness and style.	$\eta = \frac{\sum_{rs} G_{rs}}{M}$ (22) where η represents a medium.
Standard Deviation	It shows the image's contrast and the differences between each pixel and the central pixels.	$\alpha = \sqrt{\frac{\sum_{rs}(G_{rs}-\eta)^2}{M}}$ (23) where α represents a standard deviation.
Asymmetry	it denotes a measurement where the values' intensity is	$\beta = \frac{\sum_{rs}(G_{rs}-\eta)^3}{M\alpha^3}$ (24) where β represents an asymmetry.

	not symmetrical for the medium.	
Kurtosis	It gauges how closely the intensity distribution resembles a normal distribution, whether it is maximum or flat.	$\delta = \frac{\sum_{rs} (G_{rs} - \eta)^4}{(\mathrm{M} - 1)\alpha^4}$ (25) where δ represents a standard deviation.

2.5 Model Formulation

The proposed classification framework is developed using a multi-class Suport Vector Machine (SVM) model optimised through advanced metaheuristic algorithms Let the dataset be denoted as $D = \{(x_i, y_i)\}_{i=1}^{N}$, where $x_i \in \mathbb{R}^d$ represents the extracted feature vector comprising colour, texture, and shape descriptors, and $y_i \in \{1, 2, \ldots, K\}$ represents the class label. This study categorises skin into K=9, indicating normal skin and eight distinct skin disease categories. A One-vs-All (OvA) strategy is employed for multi-class classification as represented in equation 26. For each class k, a binary SVM classifier is developed to differentiate samples of class k from all other classes. The decision function for each classifier is characterised as a linear combination of transformed feature inputs in a high-dimensional space, with the ultimate class label allocated according to the highest decision score among all classifiers.

The SVM model seeks to minimise a structural risk function that balances margin maximisation and classification error. This is accomplished by minimising a regularised objective function, represented by equation 27, which consists of two components: a margin term that enforces class separation and a penalty term that addresses misclassification errors via slack variables. A Radial Basis Function (RBF) kernel, represented by equation 29, is used to transform input features into a nonlinear space, allowing the model to effectively capture the intricate relationships present in dermoscopic image data. The efficacy of the SVM model is significantly influenced by two essential hyperparameters: the regularisation parameter C and the kernel parameter γ. The optimal values of these hyperparameters are determined by formulating the problem as a constrained optimisation task, represented by equations 30-32, to minimise the classification error assessed through 10-fold cross-validation. The optimisation process examines specified limits for C and γ, ensuring that the chosen parameters achieve optimal generalisation performance while preventing overfitting. The ultimate optimal solution pertains to the parameter configuration that minimises the average cross-validation error.

2.5.1 Problem Formulation

Let the dataset be represented as:

$D = \{(x_i, y_i)\}$, for $i = 1, 2, \ldots, N$ (25)

Where:

- $x_i \in \mathbb{R}^d$ represents the extracted feature vector (colour, texture, shape features)
- $y_i \in \{1, 2, \ldots, K\}$ represents the class label
- N is the total number of samples

- K = 9 classes (Normal + 8 skin diseases)

2.5.2 Multi-Class SVM Model

A One-vs-All (OvA) strategy is used.
For each class k, the decision function is:

$$f_k(x) = w_k^T \varphi(x) + b_k \quad (26)$$

Where:

- w_k = weight vector
- b_k = bias
- $\varphi(x)$ = nonlinear feature mapping

The predicted class is:

$$\hat{y} = \text{argmax}_k \, f_k(x)$$

2.5.3 SVM Objective Function

The optimisation problem aims to minimise:

$$(1/2) \, ||w||^2 + C \times \Sigma \, \xi_i \quad (27)$$

Subject to the constraints:

$$y_i \, (w^T \varphi(x_i) + b) \geq 1 - \xi_i \quad (28)$$

$$\xi_i \geq 0$$

Where:

- C = regularisation parameter
- ξ_i = slack variables (penalty for misclassification)

2.5.4 Kernel Function

The Radial Basis Function (RBF) kernel is used:

$$K(x_i, x_j) = \exp(-\gamma \, ||x_i - x_j||^2) \quad (29)$$

Where:

- γ = kernel parameter controlling decision boundary flexibility

2.5.5 Hyperparameter Optimisation Objective

The goal is to find optimal parameters:

$$\theta = (C, \gamma) \quad (30)$$

The optimisation objective is:
Minimise:

$$F(\theta) = 1 - \text{Accuracy}(\theta) \quad (31)$$

Using 10-fold cross-validation:

$$F(\theta) = (1 / Kf) \times \Sigma \, [1 - \text{Accuracy}_j(\theta)] \quad (32)$$

Where:

- Kf = 10 folds

Constraints

$$C\_min \leq C \leq C\_max$$

$$\gamma\_min \leq \gamma \leq \gamma\_max$$

2.5.6 Hyperparameter Settings

Hyperparameters: RBF-SVM with $C \in [10^{-3},10^{3}]$, $\gamma \in [10^{-4},10^{1}]$; population size = 30; iterations = 100; 10-fold cross-validation; 90:10 train-test split. EAO uses SCF, FROBLAO, and GM; EHHO uses adaptive weights, DLH, and DBO-based update.

2.6 Algorithm for the Model

Algorithms 2 and 3 outline the procedures for executing the EAO-MCMLMBSVM and EHHO-MCMLMBSVM models, respectively.

2.6.1 EAO-MCMLMBSVM Algorithm 2 (Enhanced AO)

Steps:

1. Initialise a population of candidate solutions:
   $\theta_i = (C, \gamma)$
2. Evaluate fitness using cross-validation error
3. While the stopping condition is not met:
   - Apply Search Control Factor (SCF) to balance exploration and exploitation
   - Update candidate solutions (global + local search)
   - Apply Fast Random Opposition-Based Learning (FROBLAO):
     $\theta' = a + b - \theta$
   - Apply Gaussian Mutation (GM):
     $\theta = \theta + N(0, \sigma^2)$
   - Evaluate new solutions
   - Select the best solution
4. Output optimal parameters θ^*

2.6.2 EHHO-MCMLMBSVM Algorithm 3 (Enhanced HHO)

Steps:

1. Initialise population:
   $\theta_i = (C, \gamma)$
2. Evaluate fitness
3. While the stopping condition is not met:
   - Update adaptive weights (w_1, w_2)
   - Perform exploration and exploitation phases
   - Apply Dimension Learning-Based Hunting (DLH)
   - Apply DBO-inspired position update
   - Update candidate solutions
   - Evaluate fitness
   - Select the best solution
4. Output optimal parameters θ^*

2.6.3 Description of the EHHO-MCMLMBSVM Algorithm

The MCMLMBSVM-EAO model commences by initialising a population of candidate solutions, with each solution representing a pair of SVM hyperparameters: the regularisation parameter and the kernel parameter. The fitness of each candidate is assessed through the classification error obtained from 10-fold cross-validation. In each iteration, the Aquila Optimiser refines candidate solutions by dynamically balancing global exploration and local exploitation via the integration of a Search Control Factor. To augment diversity and avert premature convergence, Fast Random

Opposition-Based Learning is employed, facilitating the concurrent assessment of candidate solutions and their respective opposite positions within the search space. A Gaussian Mutation mechanism is implemented to enhance local search near high-quality solutions, thus augmenting the accuracy of hyperparameter tuning. The optimisation process proceeds iteratively, with candidate solutions being refined and assessed until a termination criterion is met. The most effective solution is chosen as the optimal hyperparameter configuration, which is then utilised to train the final multi-class SVM classifier.

2.6.3 Description of the EHHO-MCMLMBSVM Algorithm

The MCMLMBSVM-EHHO model adheres to a comparable optimisation framework, utilising an improved Harris Hawks Optimiser to direct the search process. A population of candidate hyperparameter solutions is generated and assessed using cross-validation error. In each iteration, the algorithm refines candidate solutions employing a Double Adaptive Weights Strategy that dynamically adjusts the balance between exploration and exploitation phases to guarantee stable convergence. The Dimension Learning-Based Hunting mechanism is implemented to enhance information exchange across various dimensions of the search space, thus improving search coverage and solution diversity. Additionally, a position update strategy derived from the Dung Beetle Optimiser is employed to enhance local search efficacy while preserving population diversity. The iterative optimisation continues until the convergence criteria are satisfied, at which point the optimal candidate solution is chosen. The optimal parameter set is utilised to train the final SVM model for multi-class skin disease classification.

3. RESULTS AND DISCUSSION OF THE FINDINGS

This section presents a detailed description of the experimental methodology and the corresponding results. Two classification models, EAO-MCMLMBSVM and EHHO-MCMLMBSVM, were developed and evaluated using 10-fold cross-validation. This validation technique entails partitioning the dataset into ten equal segments, wherein the model is trained on nine segments and assessed on the remaining segment. This procedure is performed ten times, enabling each subset to serve as the test set once, thus ensuring a reliable and unbiased performance evaluation. The Multi-Class Enhanced Machine Learning Model based on Support Vector Machine (MCMLMBSVM) was optimised using two sophisticated metaheuristic algorithms: the Enhanced Aquila Optimiser (EAO) and the Enhanced Harris Hawks Optimiser (EHHO). All experiments were conducted on a Windows 11 (64-bit) system equipped with an Intel Core i3-1005G1 processor (1.20 GHz) and 8 GB of RAM, utilising MATLAB R2020a as the implementation platform. The effectiveness of the proposed models was evaluated using several standard metrics, including false positive rate, specificity, sensitivity, precision, and accuracy, to assess their performance in classifying different categories of skin cancer lesions. The results obtained from these evaluations are summarised in Tables 3-5.

3.1 Performance Evaluation Metrics of the Classification Model of the EAO-MCMLMBSVM on the Skin Datasets

The data in Table 3 demonstrate that Actinic Keratosis (ACK) skin disease datasets displayed the highest misclassification rates relative to other Skin disease datasets. The EAO-MCMLMBSVM model inaccurately categorises 20 diseased skin image samples as healthy and misclassifies 18 healthy samples as diseased. A comprehensive analysis of the eight skin disease categories (DEM, BEK, ACK, MEM, PSO, SCA, BCC, and ECZ) reveals that the ACK dataset demonstrated the highest rate of misclassification.

Table3. Performance evaluation metrics of the classification model of the EAO-MCMLMBSVM on skin datasets

Classes of the Diseased Dataset	True Positive (TP)	False Negative (FN)	False Positive (FP)	True Negative (TN)
All Skin Diseased Dataset	1980	20	18	682
DEM	244	6	7	693
BEK	242	8	9	691
ACK	239	11	11	689
MEM	245	5	6	694
PSO	246	4	7	693
SCA	242	8	8	692
BCC	245	5	6	694
ECZ	242	8	10	690

Note:
"Dermatofibroma (DEM)", "Benign Keratosis (BEK)", "Actinic Keratosis (ACK)", "Melanoma (MEM)", "Psoriasis (PSO)", "Scabies (SCA)", "Basal Cell Carcinoma (BCC)", "Eczema or Atopic Dermatosis (ECZ)", Average (AVE), "Enhanced Aquila Optimser-Support Vector Machine (EAO-SVM)"

3.2 Performance Evaluation Metrics of the Classification Model of the EHHO-MCMLMBSVM on the Skin Datasets

The data in Table 4 demonstrate that Actinic Keratosis (ACK) skin disease datasets displayed the highest misclassification rates relative to other Skin disease datasets. The EHHO-MCMLMBSVM model inaccurately categorises 18 diseased skin image samples as healthy and misclassifies 16 healthy samples as diseased. A comprehensive analysis of the eight skin disease categories (DEM, BEK, ACK, MEM, PSO, SCA, BCC, and ECZ) reveals that the ACK dataset demonstrated the highest rate of misclassification.

Table 4. Performance evaluation metrics of the classification model of the EHHO-MCMLMBSVM on skin datasets

Classes of the Diseased Dataset	True Positive (TP)	False Negative (FN)	False Positive (FP)	True Negative (TN)
All Skin Diseased Dataset	1982	18	16	684
DEM	245	5	6	694
BEK	243	7	8	692
ACK	240	10	9	691
MEM	245	5	5	695
PSO	246	4	6	694
SCA	244	6	7	693
BCC	245	5	5	695
ECZ	244	6	8	692

Note:
"Dermatofibroma (DEM)", "Benign Keratosis (BEK)", "Actinic Keratosis (ACK)", "Melanoma (MEM)", "Psoriasis (PSO)", "Scabies (SCA)", "Basal Cell Carcinoma (BCC)", "Eczema or Atopic Dermatosis (ECZ)", Average (AVE), "Enhanced Harris Hawk Optimiser-Support Vector Machine (EHHO-SVM)"

3.3 Performance Evaluation Metrics of the Developed Multi-Class Machine Learning Models Based on Support Vector Machine (EAO-MCMLMBSVM and EHHO-MCMLMBSVM) on Skin Disease Dataset

The EAO-MCMLMBSVM model generated false positive rate (FPR) values of 1.00%, 1.29%, 1.57%, 0.86%, 1.00%, 1.14%, 0.86%, and 1.43%, while the EHHO-MCMLMBSVM model produced marginally lower FPR values of 0.86%, 1.14%, 1.29%, 0.71%, 0.86%, 1.00%, 0.71%, and 1.14% for the disease categories DEM, BEK, ACK, MEM, PSO, SCA, BCC, and ECZ, respectively. The EAO-MCMLMBSVM approach achieved specificity rates of 99.00%, 98.71%, 98.43%, 99.14%, 99.00%, 98.86%, 99.14%, and 98.57%, whereas the EHHO-MCMLMBSVM model recorded marginally superior values of 99.14%, 98.86%, 98.71%, 99.29%, 99.14%, 99.00%, 99.29%, and 98.86% for the identical class set. The EAO-MCMLMBSVM model achieved sensitivity scores of 97.60%, 96.80%, 95.60%, 98.00%, 98.40%, 96.80%, 98.00%, and 96.80%. The EHHO-MCMLMBSVM variant attained results of 98.00%, 97.20%, 96.00%, 98.00%, 98.40%, 97.60%, 98.00%, and 97.60%. A comparable trend was noted in precision, with EAO-MCMLMBSVM yielding scores of 97.21%, 96.41%, 95.60%, 97.61%, 97.23%, 96.80%, 97.61%, and 96.03%, while EHHO-MCMLMBSVM achieved superior precision scores of 97.61%, 96.81%, 96.39%, 98.00%, 97.62%, 97.21%, 98.00%, and 96.83%. The EAO-MCMLMBSVM framework attained overall classification accuracies of 98.63%, 98.21%, 97.68%, 98.84%, 98.84%, 98.32%, 98.84%, and 98.11%. In contrast, the EHHO-MCMLMBSVM model exhibited marginally superior performance with accuracies of 98.84%, 98.42%, 98.00%, 98.95%, 98.95%, 98.63%, 98.95%, and 98.53% across the eight disease categories (DEM, BEK, ACK, MEM, PSO, SCA, BCC, and ECZ), as detailed in Table 5. The results in Tables 7 and 9 demonstrate that the EAO-MCMLMBSVM and EHHO-MCMLMBSVM classification models are statistically significant, with all performance metric p-values falling below the 0.05 significance threshold.

Table 5. Performance evaluation metrics of the developed multi-class machine learning models based on support vector machine (EAO-MCMLMBSVM and EHHO-MCMLMBSVM) on skin disease dataset

	All Diseased Datasets	DEM	BEK	ACK	MEM	PSO	SCA	BCC	ECZ	AVE
False Positive Rate (FPR) (%)										
EAO-MCMLMBSVM	2.57	1.00	1.29	1.57	0.86	1.00	1.14	0.86	1.43	1.30
EHHO-MCMLMBSVM	2.29	0.86	1.14	1.29	0.71	0.86	1.00	0.71	1.14	1.11
Specificity (%)										
EAO-MCMLMBSVM	97.43	99.00	98.71	98.43	99.14	99.00	98.86	99.14	98.57	98.70
EHHO-MCMLMBSVM	97.71	99.14	98.86	98.71	99.29	99.14	99.00	99.29	98.86	98.89
Sensitivity (%)										
EAO-MCMLMBSVM	99.00	97.60	96.80	95.60	98.00	98.40	96.80	98.00	96.80	97.44

EHHO-MCMLMBSVM Precision (%)	99.10	98.00	97.20	96.00	98.00	98.40	97.60	98.00	97.60	97.77
EAO-MCMLMBSVM	99.10	97.21	96.41	95.60	97.61	97.23	96.80	97.61	96.03	97.07
EHHO-MCMLMBSVM Accuracy (%)	99.20	97.61	96.81	96.39	98.00	97.62	97.21	98.00	96.83	97.52
EAO-MCMLMBSVM	98.59	98.63	98.21	97.68	98.84	98.84	98.32	98.84	98.11	98.45
EHHO-MCMLMBSVM	98.74	98.84	98.42	98.00	98.95	98.95	98.63	98.95	98.53	98.67

Note:
Dermatofibroma (DEM), Benign Keratosis (BEK), Actinic Keratosis (ACK), Melanoma (MEM), Psoriasis (PSO), Scabies (SCA), Basal Cell Carcinoma (BCC), Eczema (ECZ), Average (AVE), Enhanced Aquila Optimiser-Multi-Class Enhanced Machine Learning Model Based on Support Vector Machine (EAO-MCMLMBSVM), Enhanced Harris Hawk Optimiser-Multi-Class Enhanced Machine Learning Model Based on Support Vector Machine (EHHO-MCMLMBSVM)

Table 6. One-sample Statistics of the EAO-MCMLMBSVM model on skin datasets

	N	Mean	Std. Deviation	Std. Error Mean
False Positive Rate	36	2.5000	.93988	.15665
Specificity	36	97.5000	.93988	.15665
Sensitivity	36	94.6972	2.46571	.41095
Precision	36	94.1036	2.63782	.43964
Accuracy	36	96.8987	1.15039	.19173

Table 7. One-sample t-test of the EAO-MCMLMBSVM model on skin datasets

	t	df	Sig. (2-tailed)	Mean Difference	95% Confidence Interval of the Difference	
					Lower	Upper
False Positive Rate	15.959	35	.000	2.50000	2.1820	2.8180
Specificity	622.417	35	.000	97.50000	97.1820	97.8180
Sensitivity	230.434	35	.000	94.69722	93.8629	95.5315
Precision	214.048	35	.000	94.10357	93.2111	94.9961
Accuracy	505.387	35	.000	96.89869	96.5095	97.2879

Table 8. One-sample statistics of the EHHO-MCMLMBSVM model on skin datasets

	N	Mean	Std. Deviation	Std. Error Mean
False Positive Rate	36	2.2381	.90222	.15037
Specificity	36	97.7619	.90222	.15037
Sensitivity	36	95.3194	2.22014	.37002
Precision	36	94.7536	2.42574	.40429
Accuracy	36	97.2456	1.05527	.17588

Table 9. One-sample t-test of the EHHO-MCMLMBSVM model on skin datasets

	t	df	Sig. (2-tailed)	Mean Difference	95% Confidence Interval of the Difference	
					Lower	Upper
False Positive Rate	14.884	35	.000	2.23810	1.9328	2.5434
Specificity	650.145	35	.000	97.76190	97.4566	98.0672
Sensitivity	257.603	35	.000	95.31944	94.5683	96.0706
Precision	234.371	35	.000	94.75362	93.9329	95.5744
Accuracy	552.911	35	.000	97.24556	96.8885	97.6026

3.4 Graphical Representation of Performance Evaluation Metrics of the EAO-MCMLMBSVM and EHHO-MCMLMBSVM Classification Models on Skin Datasets

The graphical representation of the evaluation metrics in Figure 2 indicates that the EAO-MCMLMBSVM model achieved its best performance on the MEM and BCC datasets when compared with the DEM, BEK, ACK, PSO, SCA**,** and ECZ datasets across most of the assessed metrics. As shown in Figure 2, the EAO-MCMLMBSVM model exhibited the next highest level of performance on the PSO dataset, whereas the EAO-MCMLMBSVM model exhibited the lowest level of performance on the ACK dataset among the evaluated classes. Similarly, the graphical depiction of the evaluation metrics in Figure 3 demonstrates that the EHHO-MCMLMBSVM model attained optimal performance on the MEM and BCC datasets in comparison to the DEM, BEK, ACK, PSO, SCA, and ECZ datasets across the majority of the evaluated metrics. Figure 3 illustrates that the EHHO-MCMLMBSVM model demonstrated the next highest performance on the PSO dataset, while it exhibited the lowest performance on the ACK dataset among the assessed categories.

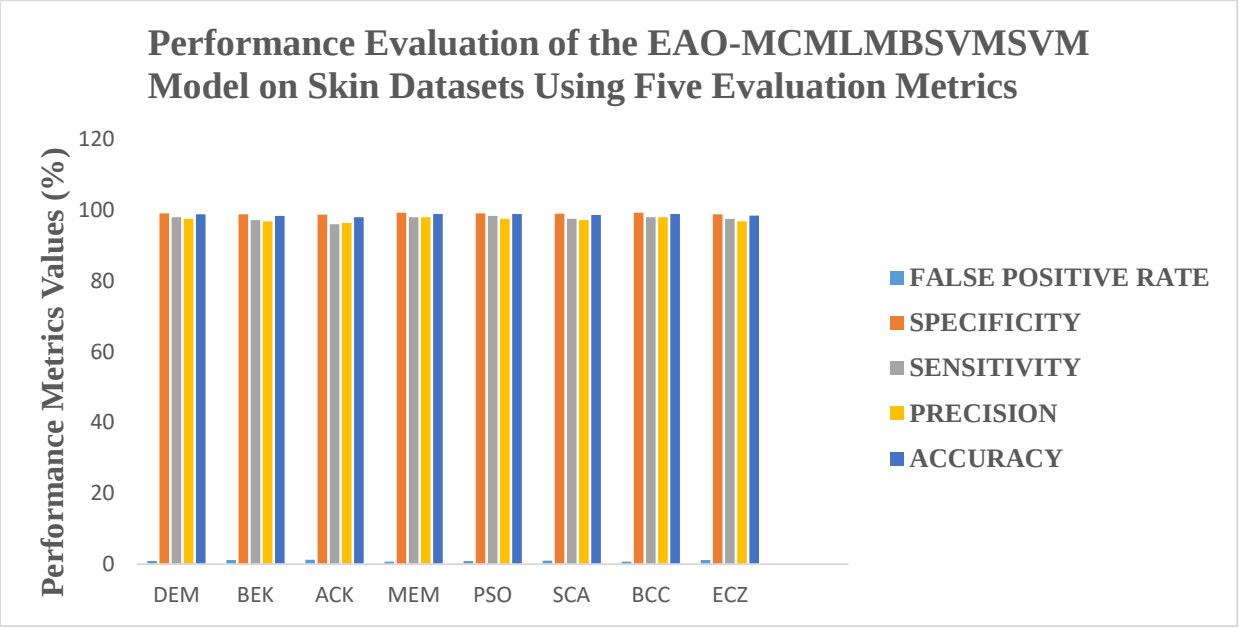

Figure 2. Performance evaluation outcomes of the EAO-MCMLMBSVM classification model on skin datasets

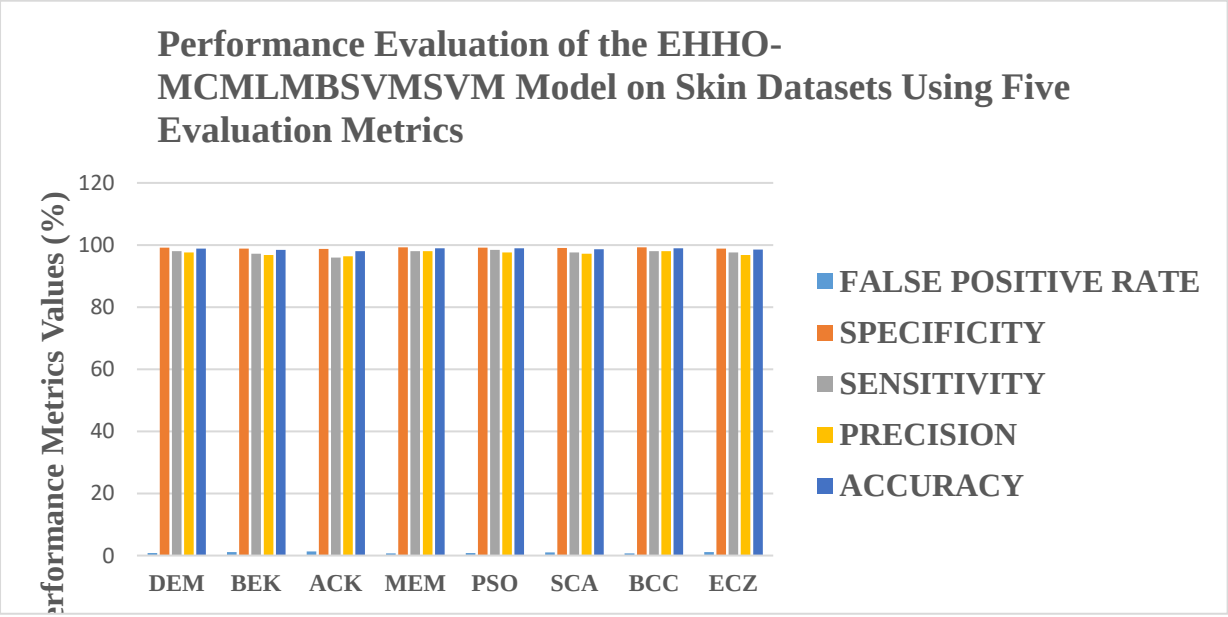

Figure 3. Performance evaluation outcomes of the EHHO-MCMLMBSVM classification model on sin datasets

3.5 Comparison of Performance Evaluation Metrics for the Developed Multi-Class Enhanced Machine Learning Models Based on Support Vector Machine (EAO-MCMLMBSVM and EHHO-MCMLMBSVM) with the Existing Classification Models on Skin Diseases Classifications

Table 8 indicates that the proposed enhanced Support Vector Machine models (EAO-MCMLMBSVM and EHHO-MCMLMBSVM) surpassed the traditional AO-SVM and HHO-SVM models across all evaluation metrics employed in this study. Also, the improved models exhibit enhanced performance relative to various existing machine learning methods across the evaluated metrics. Specifically, both models surpass the SVM-BWO model reported in [35], in addition to the SVM, RF, and KNN models presented in [9]. They also exhibit enhanced outcomes compared to the Hybrid Features Optimised MSVM model presented in [37] and the RF, NB, GB, and DT models proposed in [45]. The developed models demonstrate superior performance compared to several advanced deep learning methodologies, such as ResNet, DenseNet, and Xception models reported in [32], the AlexNet model introduced in [33], the CNN One-versus-All framework proposed in [34], the DCNN model outlined in [1], the GoogleNet-WELM-DSSA methodology developed in [36], the VGG16 model presented in [49], and the CNN model introduced in [50]. However, some cutting-edge methodologies continue to surpass the proposed EAO-MCMLMBSVM and EHHO-MCMLMBSVM models in some particular metrics. The FOA-SVM optimised model presented in [38] achieves superior sensitivity and accuracy; however, it does not exceed the proposed models regarding specificity. The AlexNet model presented in [31] attains superior scores on the majority of evaluation metrics, with the exception of the false positive rate. Similarly, the SVC model in [45] demonstrates superior performance across all metrics, with the exception of sensitivity. The AlexNet-SVM hybrid model proposed in [43] exhibits enhanced sensitivity and precision, despite a lower accuracy. A comprehensive comparison of these results is summarised in Table 8.

Table 8. Comparison of performance evaluation metrics for the developed multi-class enhanced machine learning models based on support vector machine (EAO-MCMLMBSVM and EHHO-MCMLMBSVM) with the existing classification models on skin disease classifications

Author(s) and Models	False Positive Rate (%)	Specificity (%)	Sensitivity (%)	Precision (%)	Accuracy (%)
		[31]			
"AlexNet"	-	98.93	98.33	97.73	98.61
		[32]			
"ResNet"	-	96.00	-	77.00	78.10
"DenseNet"	-	97.00	-	80.00	81.90
"Xception"	-	98.0	-	74.00	81.80
		[33]			
"AlexNet"	-	88.00	81.00	82.20	84.00
		[34]			
"CNN with One-Versus-All"	-	-	93.56	96.57	91.44
		[1]			
"DCNN"	-	-	93.66	96.57	91.43
		[35]			
"SVM-BWO"	-	78.00	76.00	78.00	92.00
		[8]			
"Support Vector Machine (SVM)"	-	-	97.57	97.71	97.00
'K-Nearest Neighbour (KNN)"	-	-	95.57	95.71	95.00
"Decision Tree (DT)"	-	-	95.14	95.14	95.00

		[36]			
"Random Forest (RF)"	-	-	94.00	94.00	87.00
"Decision Tree (DT)"	-	-	74.00	75.00	68.00
"Logistic Regression (LR)"	-	-	55.00	56.00	58.00
"Support Vector Machine (SVM)"	-	-	50.00	54.00	53.00
"K-Nearest Neighbour (KNN)"	-	-	50.00	54.00	48.00
		[9]			
"Support Vector Machine (SVM)"	-	-	90.80	91.00	90.70
"Random Forest (RF)"	-	-	84.20	84.80	84.20
"K-Nearest Neighbour (KNN)"	-	-	67.10	72.80	67.10
		[37]			
"Hybrid Features Optimised MSVM"	-	97.26	96.20	-	98.00
		[38]			
"Fruit Fly Optimisation-Support Vector Machine (FOA-SVM)"	-	96.00	98.50	-	98.80
		[39]			
"GoogleNet-WELM-DSSA"	-	96.68	96.40	87.49	97.25
		[40]			
"GAN-Improved MobileNetV2 (G-DMN)"	-	77.26	96.19	75.28	80.13
		[41]			
"ESVMKRF-HEAO"	-	96.00	95.90	96.30	97.40
		[42]			
"ANN-GWO"	-	-	95.58	94.18	97.10
		[43]			
"AlexNet-SVM"	-	-	98.23	98.23	98.32
		[44]			
"HFB-CNN-BiLSTM"	-	95.19	95.41	95.23	96.68
		[45]			
"Support Vector Classifier (SVC)"	-	100.0	96.00	100.00	99.30
"Random Forest (RF)	-	87.70	90.00	94.00	97.91
"Naïve Bayes (NB)"	-	90.50	60.00	100.00	85.41
"Gradient Boosting (GB)"	-	86.90	95.00	97.00	95.83
"Decision Tree (DT)"	-	87.40	74.00	94.00	95.13
		[46]			
"Wolf AntLion Neural Network (WALNN)"	-	98.34	99.12	98.98	99.01
		[47]			
"MCTHKSVM"	-	-	98.50	98.41	98.78
		[48]			
"SWNet"	-	100.00	99.90	100.00	99.86
		[49]			
"VGG16"	2.01	97.99	93.10	88.70	93.29
		[50]			
"CNN"	-	88.45	82.05	-	93.43

		[51]			
"AO-SVM"	3.00	97.00	93.33	92.85	96.18
"HHO-SVM"	2.57	97.43	94.37	93.92	96.76
		Developed Classification Model			
MCMLMBSVM-EAO	**1.30**	**98.70**	**97.44**	**97.07**	**98.45**
MCMLMBSVM-EHHO	**1.11**	**98.89**	**97.77**	**97.52**	**98.67**

Note: Histogram Oriented Gradient (HOG), Aquila Optimiser-Support Vector Machine (AO-SVM), Harris Hawk Optimiser-Support Vector Machine (HHO-SVM), Multi-Class Transductive Hybrid Kernel Support Vector Machine (MCTHKSVM), SkinWiseNet (SWNet), Support Vector Machine-Black Widow Optimisation (SVM-BWO), Ensemble Support Vector Machine Kernel Random Forest-Based Hybrid Equilibrium Aquila Optimisation (ESVMKRF-HEAO), Deep Convolutional Neural Network (DCNN), GoogleNet-Weighted Extreme Learning Machine Dynamic Salp Swarm Algorithm (GoogleNet-WELM-DSSA), Generated Adversarial Network-Dense-MobileNetV2 (G-DMN), Hybrid Flash Butterfly Optimised Convolutional Neural Network with Bidirectional Long Short-Term Memory (HFB-CNN-BiLSTM), Artificial Neural Network-Grey Wolf Optimisation (ANN-GWO), Multi-Class Enhanced Machine Learning Model Based on Support Vector Machine-Enhanced Aquila Optimiser (MCMLMBSVM-EAO), Multi-Class Enhanced Machine Learning Model Based on Support Vector Machine-Enhanced Harris Hawk Optimiser (MCMLMBSVM-EHHO)

3.6 Discussion of the Findings

Table 8 indicates that the improved SVM models (EAO-MCMLMBSVM and EHHO-MCMLMBSVM) surpassed traditional AO-SVM, HHO-SVM, and other classifiers, including SVM-BWO, SVM, RF, and KNN, Optimised MSVM, and the RF, NB, GB, and DT, in all evaluation metrics. While enhancements to the standard Aquila Optimiser (AO) augment convergence speed and robustness in AO-SVM implementations, single-algorithm frameworks intrinsically restrict the equilibrium between exploration and exploitation, thereby constraining global search efficacy [52]. Likewise, alterations to traditional Harris Hawks Optimisation (HHO) enhance local search stability and convergence accuracy. Nonetheless, in the context of intricate and high-dimensional optimisation landscapes, the standalone Harris Hawks Optimisation (HHO) is susceptible to premature convergence and inadequate population diversity, as it often fails to effectively balance exploration and exploitation, leading to stagnation or entrapment in local optima within high-dimensional search spaces [53, 54, 55]. The improved SVM models (EAO-MCMLMBSVM and EHHO-MCMLMBSVM) attain expedited convergence, enhanced stability, and superior hyperparameter optimisation by integrating the complementary advantages of AO's varied exploration strategy with HHO's adaptive exploitation mechanism, thus addressing the shortcomings of singular metaheuristic methods and more effectively balancing the exploration-exploitation trade-off [56, 57-58]. The optimisation enhancements directly enhance the classification efficacy of the Support Vector Machine (SVM) in multiclass learning contexts, as enhanced metaheuristics provide a better balance between exploring new possibilities and using existing knowledge, while also optimising features and reducing the chance of settling on a suboptimal solution too soon [59-60]. As a result, optimising feature subsets and classifier parameters at the same time leads to clearer decision boundaries, along with better precision, recall, and F1-scores [61-62]. Diversification strategies mitigate the risk of convergence to local optima, resulting in more stable performance across complex, high-dimensional datasets [63–65.

Moreover, Table 8 illustrates that EAO-MCMLMBSVM surpassed EHHO-MCMLMBSVM, despite employing an identical methodological framework. This distinction arises from variations in their foundational metaheuristic search strategies, whose optimisation behaviour profoundly influences SVM parameter selection. The Aquila Optimiser prioritises broad global exploration over localised exploitation, which could potentially cause premature convergence within complex hyperparameter landscapes [66]. Conversely, the Harris Hawks Optimiser employs adaptive switching between exploration and exploitation phases, thereby improving both accuracy and stability during parameter refinement [67]. Furthermore, the No Free Lunch theorem posits that no single optimisation algorithm demonstrates superiority across all problem domains [68-69]. Consequently, EHHO may have discerned more suitable SVM hyperparameters for heterogeneous datasets, while EAO may have reached suboptimal solutions under identical experimental conditions. In addition, Figures 2 and 3 indicate that both advanced classification models (EAO-MCMLMBSVM and EHHO-MCMLMBSVM) exhibited superior performance on melanoma (MEM) and basal cell carcinoma (BCC) skin datasets compared to other skin disease datasets. This discrepancy may be elucidated by the attributes of the data. Typical skin images exhibit more uniform feature distributions and enhanced class separability, facilitating more discriminative decision boundaries [70]. The images of other skin disease datasets, especially actinic keratosis (ACK), show significant variation, with irregular lesion patterns and overlapping features. Such variation increases the chance of misclassification [71-72]. Even though each class has 250 samples, the complex structure of ACK skin images makes it difficult to define boundaries. This requires advanced feature extraction and robust classification methods. The relative uniformity of both MEM and BCC skin images allows EAO-MCMLMBSVM and EHHO-MCMLMBSVM to attain superior accuracy, sensitivity, and precision [71-72].

Furthermore, the findings in Table 8 indicate that both advanced classification models (EAO-MCMLMBSVM and EHHO-MCMLMBSVM) surpassed various other machine learning and deep learning methods, which is attributable to its enhanced optimisation capacity and generalisation efficacy. Recent empirical literature indicates that the integration of metaheuristic optimisers with machine learning classifiers enhances hyperparameter search efficacy, mitigates the risk of local optima entrapment, and yields models that generalise more effectively across varied datasets compared to conventional tuning methods [73-74]. The SVM-BWO model from [38] employed singular metaheuristic optimisation strategies, potentially constraining search diversity and diminishing robustness in intricate dermatological feature spaces. Nevertheless, single-strategy metaheuristics frequently exhibit a limited balance between exploration and exploitation, rendering them more susceptible to converging on local optima compared to hybrid or multi-strategy approaches, which preserve greater solution diversity and robustness [73, 75-76]. In a similar vein, when comparing the EAO-MCMLMBSVM and EHHO-MCMLMBSVM models with deep learning architectures like ResNet, DenseNet, and Xception, as proposed by the authors in [32], alongside the DCNN model developed by the authors in [1], the EAO-MCMLMBSVM and EHHO-MCMLMBSVM models exhibit superior generalisation on moderately sized datasets due to the structural efficacy of support vector machines in high-dimensional spaces and their reduced susceptibility to overfitting in scenarios with limited data. Support Vector Machines (SVMs) are esteemed for their resilience and proficiency in generalising effectively from small to medium-sized training datasets, whereas deep neural networks typically necessitate extensive annotated datasets and considerable model complexity to prevent inadequate generalisation and overfitting on constrained data. When these datasets are inadequate, their performance may decline due to heightened overfitting and diminished generalisation ability, a

well-documented issue in the literature concerning deep learning data scarcity and its effects on model performance [77-78].

In contrast, certain sophisticated machine learning models surpassed the EAO-MCMLMBSVM and EHHO-MCMLMBSVM The MCTHKSVM model created by the authors [47] likely utilised multi-kernel learning mechanisms, that more effectively represented varied feature distributions than single-kernel SVM methods, thereby enhancing classification accuracy in intricate lesion datasets [79]. The WALNN model introduced by the authors in [46] likely attained superior outcomes due to its adaptive neural weighting mechanisms, which facilitate dynamic parameter adjustments during training, thereby enhancing nonlinear mapping and deeper feature abstraction, particularly in the presence of significant dataset variability. Adaptive weighting and dynamic parameter adjustment strategies enhance neural network flexibility and generalisation capabilities relative to static weight methods, enabling the model to prioritise salient information and discern complex patterns in heterogeneous data [80-81]. Likewise, specific deep learning models surpassed EAO-MCMLMBSVM and EHHO-MCMLMBSVM models owing to their domain-specific architectural benefits and transfer learning methodologies, which allowed them to better adapt to the unique characteristics of the datasets they were trained on and improve overall performance in tasks such as image classification and pattern recognition. The SWNet model developed by the authors in [48] likely integrated specialised convolutional blocks and feature fusion mechanisms designed for dermatological texture patterns, enabling it to acquire more discriminative hierarchical features than conventional SVM-based classifiers, especially when trained on adequately large and diverse datasets. Deep CNN architectures, characterised by multi-path feature extraction and extensive network design, have demonstrated superior capability in capturing intricate local and global patterns in skin lesion images compared to shallow or manually designed models [82-83]. Moreover, the AlexNet model created by the authors in [31] may have employed transfer learning from extensive datasets, such as ImageNet, which facilitates the use of pre-trained feature extractors and consequently enhances classification efficacy in medical image analysis tasks. Transfer learning utilising ImageNet-pretrained CNNs has been extensively shown to enhance convergence speed and accuracy in medical imaging tasks with limited annotated training data [84-85]. The performance disparities between the EAO-MCMLMBSVM and EHHO-MCMLMBSVM models, among others, can be attributed to variations in optimisation robustness, kernel design, architectural depth, feature representation capability, dataset size, and the application of transfer learning. Although enhanced metaheuristic-based SVM models exhibit significant optimisation stability and generalisation capability, neural architectures featuring multi-kernel learning, adaptive weighting mechanisms, or deep hierarchical representation may surpass them when bolstered by extensive and varied dermatological datasets.

4. CONCLUSION

This research established two advanced intelligent frameworks for skin cancer detection, MCMLMBSVM-EAO and MCMLMBSVM-EHHO, by amalgamating refined metaheuristic optimisation methods with a multi-class Support Vector Machine classifier. The proposed framework included a thorough pipeline comprising image pre-processing, lesion segmentation via the Sobel edge detection technique, and discriminative feature extraction utilising Colour Moments and Gray Level Co-occurrence Matrix (GLCM). Furthermore, enhancement mechanisms were integrated into the Aquila Optimiser (AO) and Harris Hawks Optimiser (HHO) to mitigate the shortcomings of traditional optimisation methods in hyperparameter tuning. The

experimental assessment utilising the HAM10000 dermoscopic dataset revealed that the proposed models attained enhanced classification performance relative to various existing machine learning and deep learning methodologies. MCMLMBSVM-EAO achieved an accuracy of 98.45%, whereas MCMLMBSVM-EHHO reached 98.67%, demonstrating significant predictive capability and model robustness. The enhanced performance is primarily due to the effective optimisation of SVM hyperparameters via improved exploration and exploitation of the search space, facilitated by modified metaheuristic algorithms. The results affirm that the amalgamation of sophisticated optimisation algorithms with conventional machine learning classifiers can markedly enhance diagnostic precision in automated systems for skin cancer detection. The proposed MCMLMBSVM-EAO and MCMLMBSVM-EHHO frameworks offer a dependable and effective computational method to assist dermatologists in the early diagnosis of skin cancer and clinical decision-making.

4.1 Limitations and Practical Constraints of the Study

Despite the superior performance exhibited by the proposed EAO-MCMLMBSVM and EHHO-MCMLMBSVM frameworks, several limitations and practical constraints must be recognised. Initially, while the integration of the enhanced Aquila Optimiser (AO) and Harris Hawks Optimiser (HHO) augments convergence speed, stability, and hyperparameter optimisation, the proposed models continue to rely on metaheuristic optimisation methodologies. These methods are inherently stochastic and may not reliably ensure globally optimal solutions, especially in complex and high-dimensional search spaces, which can lead to suboptimal performance in certain scenarios or datasets. Moreover, the No Free Lunch theorem posits that no singular optimisation strategy is universally superior; consequently, the efficacy of the proposed methods may differ across various datasets and problem domains. The performance variation between EAO-MCMLMBSVM and EHHO-MCMLMBSVM demonstrates that differences in search dynamics affect the quality of the chosen SVM hyperparameters.

Secondly, the dependence on manual feature extraction techniques, such as colour moments, shape descriptors, and Gray Level Co-occurrence Matrix (GLCM)-based texture features, imposes intrinsic constraints on the ability to capture intricate and hierarchical representations of dermoscopic images. Although these features are proficient in structured pattern representation, they may insufficiently capture complex variations and irregular lesion architectures, especially in difficult categories like actinic keratosis (ACK), where feature overlap and significant intra-class variability heighten the risk of misclassification. A further limitation pertains to the characteristics of the dataset. Despite the implementation of class balancing to guarantee equitable representation, the dataset size remains moderate, with a predetermined number of samples per class. This limitation may restrict the model's exposure to the complete range of variability found in real-world clinical data, consequently impacting generalisability. The relatively uniform feature distribution in specific classes, such as melanoma (MEM) and basal cell carcinoma (BCC), enhanced classification performance, while more heterogeneous classes presented greater challenges, reflecting sensitivity to data complexity.

Moreover, from a modelling perspective, employing a single-kernel SVM (RBF kernel) may limit the capacity to accurately represent varied feature distributions among distinct skin disease categories. Advanced methodologies, including multi-kernel learning frameworks, have shown enhanced adaptability in heterogeneous data contexts and may surpass single-kernel models in specific circumstances. This constraint partially elucidates the enhanced efficacy of certain

comparative models that integrate sophisticated kernel architectures or hybrid learning methodologies. The proposed optimisation frameworks entail increased computational overhead due to iterative population-based search methods and cross-validation fitness assessment. Despite the models' superior computational efficiency compared to deep learning architectures, the optimisation phase can be time-intensive, especially when applied to larger datasets or real-time clinical scenarios. This may restrict immediate applicability in time-sensitive or resource-limited contexts without additional optimisation or parallelisation strategies.

Furthermore, although the proposed models surpass various deep learning methods on moderate-sized datasets, they do not utilise deep hierarchical feature learning or transfer learning techniques. Deep convolutional neural networks (CNNs), particularly those augmented by transfer learning from extensive datasets, have exhibited exceptional proficiency in identifying intricate spatial patterns and semantic representations. Therefore, the suggested models may be surpassed in situations involving extensive, highly varied datasets where deep learning architectures can fully utilise their representational capabilities. The performance disparities noted between the proposed models and specific advanced techniques, including multi-kernel SVMs and adaptive neural network models, underscore the impact of architectural design, feature representation, and learning adaptability. The proposed frameworks prioritise optimisation, robustness, and generalisation, but may be less effective in situations that necessitate dynamic feature learning and profound abstraction.

5. IMPLICATION OF THE STUDY

The results of this study have significant implications for medical image analysis and intelligent healthcare systems. The findings underscore the efficacy of hybrid optimisation-driven machine learning frameworks in enhancing the performance of medical image classification models. The study illustrates that integrating advanced metaheuristic optimisation techniques into the Support Vector Machine classifier can markedly enhance classification accuracy, reduce false positive rates, and strengthen the reliability of automated diagnostic systems through effective hyperparameter tuning. The proposed framework provides a computationally efficient alternative to intricate deep learning architectures, especially when used with moderately large datasets like HAM10000. This result indicates that meticulously optimised traditional machine learning algorithms can compete with, and in certain instances surpass, deep learning models when suitable feature extraction and optimisation techniques are employed. The study further advances computer-aided diagnosis systems in dermatology. The superior predictive performance of the proposed models suggests that these intelligent diagnostic tools can assist dermatologists in enhancing the accuracy and promptness of skin cancer detection, thereby improving clinical decision-making and potentially decreasing mortality linked to delayed diagnosis. The study offers a methodological contribution by showcasing the successful incorporation of advanced metaheuristic optimisation algorithms, namely the enhanced Aquila Optimiser and Harris Hawks Optimiser, into machine learning frameworks. This optimisation-focused methodology can be applied to additional medical imaging applications and pattern recognition tasks that necessitate effective parameter adjustment to attain superior classification performance.

6. FUTURE WORK

Future research should focus on improving the robustness, adaptability, and clinical applicability of the proposed EAO-MCMLMBSV and EHHO-MCMLMBSVM frameworks. This entails investigating hybrid and ensemble optimisation strategies to enhance convergence, stability and

solution quality. The incorporation of deep learning methodologies, including convolutional neural networks, can enhance handcrafted features by identifying intricate and hierarchical patterns in dermoscopic images, especially for difficult disease categories. Furthermore, integrating multi-kernel learning and adaptive kernel selection into the SVM framework could enhance the representation of heterogeneous feature spaces and increase classification accuracy. Augmenting the dataset with a broader array of diverse and clinically representative samples will enhance generalisation performance. Improving computational efficiency via parallel processing, distributed optimisation, or streamlined models is crucial for real-time implementation, especially in applications like automated dermatological diagnosis, where timely decision-making is essential. Ultimately, clinical validation and the incorporation of explainable artificial intelligence methodologies will enhance interpretability, reliability, and acceptance in practical healthcare environments, thus promoting automated dermatological diagnosis.

7. ACKNOWLEDGEMENT

Our thanks to the reviewers and the editorial team for all their efforts put into making this paper a reality.

REFERENCES

Al-Sawaff, Z. H., Yahya, Y. Z., & Kandemirli, F. (2020). LabVIEW BASED TEMPERATURE CONTROL SYSTEM FOR NEONATAL INCUBATOR. Eurasian Journal of Science Engineering and Technology, 1(1), 20–26. https://www.researchgate.net/publication/345241789

Athimoolam, S. and Karuppasamy, P. (2022). “Smart incubator for premature baby in an IoT Applications,” *Journal of Semiconductor Devices and Circuits*, vol. 9, no. 2, pp. 1 –9.

[1] Ali, M. S., Miah, M. S., Haque, J., Rahman, M. M., and Islam, M. K. (2021). An enhanced technique of skin cancer classification using deep convolutional neural network with transfer learning models. *Machine Learning with Applications*, 5, 1–8.

[2] Dorj, U.-O., Lee, K.-K., Choi, J.-Y., and Lee, M. (2018). The skin cancer classification using deep convolutional neural network. *Multimedia Tools and Applications*, 77(8), 9909–9924.

[3] Okwor, V. C., Folasire, A., Okwor, C. J., Nwanko, K., Ntekim, A., and Arua, C. S. (2024). Clinico-epidemiological profile of skin cancer in South Western Nigeria. *Malawi Medical Journal*, 36(2), 62–72. https://pmc.ncbi.nlm.nih.gov/articles/PMC11970198/pdf/MMJ3602-0067.pdf

[4] IARC (2018). The global cancer observatory, Nigeria. *GLOBOCAN*. Retrieved October 20, 2019, from https://gco.iarc.fr/today/data/factsheets/populations/566-nigeria-fact-sheets.pdf

[5] Chatzilakou, E., Hu, Y., Jiang, N., and Yetisen, A. K. (2024). Biosensors for melanoma skin cancer diagnostics. *Biosensors & Bioelectronics*, 250, 1–19.

[6] Esteva, A., Kuprel, B., Novoa, R. A., Ko, J., Swetter, S. M., Blau, H. M., and Thrun, S. (2017). Dermatologist-level classification of skin cancer with deep neural networks. *Nature*, 542, 1–20.

[7] O'Sullivan, D. E., Brenner, D. R., Demers, P. A., Villeneuve, P. J., Friedenreich, C. M., and King, W. D. (2019). Indoor tanning and skin cancer in Canada: A meta-analysis and attributable burden estimation. *Cancer Epidemiology*, 59, 1–7.

[8] Ahammed, M., Al Mumun, M. D., and Uddin, M. F. (2022). A machine learning approach for skin disease detection and classification using image segmentation. *Healthcare Analytics*, 2, 1–15.

[9] Aldera, S. A., and Othman, M. T. B. (2022). A model for classification and diagnosis of skin disease using machine learning and image processing techniques. *International Journal of Advanced Computer Science and Application*, 13(5), 252–259.

[10] Bordoloi, D., Singh, V., Kaliyaperumal, K., Ritonga, M., Jawarneh, M., Kassanuk, T., and Quinonez-Choquecota, J. (2023). Classification and detection of skin disease based on machine learning and image processing evolutionary models. *Computer Assisted Methods in Engineering and Science*, 30(2), 247–256.

[11] Raju, S. M., and Shobha, K. B. (2025). Automated skin cancer detection using support vector machines: A comprehensive approach. *Heritage Research Journal*, 73(3), 1–8.

[12] Cortes, C., and Vapnik, V. (1995). Support-vector networks. *Machine Learning*, 20(3), 273–297. https://link.springer.com/content/pdf/10.1007/BF00994018.pdf

[13] Hsu, C.-W., Chang, C.-C., and Lin, C.-J. (2010). A practical guide to support vector classification. *IEEE Intelligent Systems*, 25(5), 20–27.

[14] Abualigah, L., Yousri, D., Abd Elaziz, M., Ewees, A. A., Al-qaness, M. A., and Gandomi, A. H. (2021). Aquila optimizer: A novel meta-heuristic optimization algorithm. *Computers and Industrial Engineering*, 157(11), 1–16.

[15] Yang, T., Fang, J., Jia, C., Liu, Z., and Liu, Y. (2023). An improved Harris Hawks optimization algorithm based on chaotic sequence and opposite elite learning mechanism. *PLOS ONE*, 18(2), 1–23. https://journals.plos.org/plosone/article/file?id=10.1371/journal.pone.0281636&type=printable

[16] Sharma, H., Bharali, J., Motghare, M., Arora, K., Yoon, C., and Prasad, G. (2025). Development and evaluation of hybrid Harris Hawks optimization algorithms for advanced engineering applications. *Scientific Reports*, 15, 1–111. https://www.nature.com/articles/s41598-025-23624-5.pdf

[17] Gao, B., Shi, Y., Xu, F., and Xu, X. (2022). An improved Aquila optimiser based on search control factor and mutation. *Processes*, 10, 1–27.

[18] Gopi, S., and Mohapatra, P. (2024). Fast random opposition-based learning Aquila optimization algorithm. *Heliyon*, 10, 1–31.

[19] Nadimi-Shahraki, M. H., Taghian, S., and Mirjalili, S. (2021). An improved grey wolf optimizer for solving engineering problems. *Expert Systems with Applications*, 166, 1–25.

[20] Kaur, N., Kaur, L., and Cheema, S. S. (2021). An enhanced version of Harris Hawks optimization by dimension learning-based hunting for breast cancer detection. *Scientific Reports*, 11, 1–26. https://pmc.ncbi.nlm.nih.gov/articles/PMC8578615/pdf/41598_2021_Article_1018.pdf

[21] Liu, X., Wang, Y., and Zhou, M. (2022). Dimensional learning strategy-based grey wolf optimizer for solving the global optimization problem. *Computational Intelligence and Neuroscience*, 2022, 1–31. https://pmc.ncbi.nlm.nih.gov/articles/PMC8818440/pdf/CIN2022-3603607.pdf

[22] Xue, J., and Shen, B. (2022). Dung beetle optimizer: A new meta-heuristic algorithm for global optimization. *Journal of Supercomputing*, 79, 7305–7336.

[23] Celebi, M. E., Wen, Q., Iyatomi, H., Shimizu, K., Zhou, H., and Schaefer, G. (2015). A state-of-the-art survey on lesion border detection in dermoscopy images. *Dermatology Research and Practice*, 2015, 1–18.

[24] Codella, N., Gutman, D. A., Celebi, M. E., Helba, B., Marchetti, M. A., Dusza, S., Kalloo, A., Liopyris, K., Mishra, N. K., Kittler, H., and Halpern, A. (2018). Skin lesion analysis toward melanoma detection: A challenge at the 2017 ISIC workshop. *IEEE Journal of Biomedical and Health Informatics*, 23(2), 501–512.

[25] Heidari, A. A., Mirjalili, S., Faris, H., Aljarah, I., Mafarja, M., and Chen, H. (2019). Harris Hawks optimization: Algorithm and applications. *Future Generation Computer Systems*, 97, 849–872.

[26] Padmavathi, K., and Thangadurai, K. (2016). Implementation of RGB and gray scale images in plant leaves disease detection: Comparative study. *Indian Journal of Science and Technology*, 9(6), 1–6. https://indjst.org/downloadarticle.php?Article_Unique_Id=INDJST5373&Full_Text_Pdf_Download=True

[27] Padmavathi, K., and Thangadurai, K. (2016). Implementation of RGB and gray scale images in plant leaves disease detection: Comparative study. *Indian Journal of Science and Technology*, 9(6), 1–6. https://indjst.org/downloadarticle.php?Article_Unique_Id=INDJST5373&Full_Text_Pdf_Download=True

[28] Mohammadi, S. M., Helfroush, M. S., and Kazemi, K. (2012). Novel shape-texture feature extraction for medical X-ray image classification. *International Journal of Innovative Computing, Information and Control*, 8(1B), 659–676. http://www.ijicic.org/ijicic-10-09087.pdf

[29] Sharif, M., Attique, M., Iqbal, Z., Faisal, M., Ullah, M. I., and Younus, M. (2018). Detection and classification of citrus diseases in agriculture based on optimized weighted segmentation and feature selection. *Computers and Electronics in Agriculture*, 150, 220–234.

[30] Luna-Benoso, B., Martinez-Perales, J., Cortes-Galicia, J., Flores-Cerapia, R., and Silva-Garcia, V. (2021). Detection of diseases in tomato leaves by colour analysis. *Electronics*, 10(9), 1–16. https://www.mdpi.com/2079-9292/10/9/1055

[31] Hosny, K. M., Kassem, M. A., and Foaud, M. M. (2018). Skin cancer classification using deep learning and transfer learning. In *Proceedings of the 2018 9th Cairo International Biomedical Engineering Conference (CIBEC)*, Cairo, Egypt (pp. 90–93).

[32] Rahman, Z., and Ami, A. M. (2020). A transfer learning-based approach for skin lesion classification from imbalanced data. In *2020 11th International Conference on Electrical and Computer Engineering (ICECE)* (pp. 65–68).

[33] Ameri, A. (2020). A deep learning approach to skin cancer detection in dermoscopy images. *Journal of Biomedical Physics and Engineering*, 10(6), 801–805.

[34] Polat, K., and Koc, K. O. (2020). Detection of skin diseases from dermoscopy images using the combination of convolutional neural network and one-versus-all. *Journal of Intelligent Systems*, 2(1), 80–97.

[35] Raju, D. N., Shanmugasundaram, H., and Sasikumar, R. (2021). Fuzzy segmentation and black widow-based optimal SVM for skin disease classification. *Medical & Biological Engineering & Computing*, 59, 2019–2035.

[36] Shetty, B., Fernandes, R., Rodrigues, A. P., Chengoden, R., Bhattacharya, S., and Lekshmanna, K. (2022). Skin lesion classification of dermoscopic images using machine learning and convolutional neural network. *Scientific Reports*, 12, 1–11.

[37] Kumar, A. (2023). A melanoma skin cancer diagnosis using hybrid feature-optimized MSVM classification model on dermatoscopic images. *GLIMPSE Journal of Computer Science*, 2(1), 19–24.

[38] Sonia, R., Joseph, J., Kalaiyarasi, D., Kalyani, N., Gupta, A. S. A. J. G., Ramkumar, G., Almoallim, H. S., Alharbi, S. A., and Raghavan, S. S. (2023). Segmenting and classifying skin lesions using fruit fly optimization algorithm with a machine learning framework. *Journal for Control, Measurement, Electronics, Computing and Communications*, 65(1), 217–231.

[39] Panneerselvam, R., and Balasubramaniam, S. (2023). Multi-class skin cancer classification using a hybrid dynamic salp swarm algorithm and weighted extreme learning machines with transfer learning. *Acta Informatica Pragensia*, 12(1), 141–159.

[40] Wang, H., Qi, Q., Sun, W., Li, X., Dong, B., and Yao, C. (2023). Classification of skin lesions with generative adversarial networks and improved MobileNetV2. *International Journal of Imaging Systems and Technology*, 33, 1561–1576.

[41] Kalpana, B., Reshmy, A. K., Pandi, S. S., and Dhanasekaran, S. (2023). OESV-KRF: Optimal ensemble support vector kernel random forest-based early detection and classification of skin diseases. *Biomedical Signal Processing and Control*, 85, 104779.

[42] Lai, W., Kuang, M., Wang, X., Ghafariasl, P., Sabzalian, M. H., and Lee, S. (2023). Skin cancer diagnosis using artificial neural network and improved gray wolf optimization. *Scientific Reports*, 13(1), 1–17.

[43] Sathvika, V. B. T., Anmisha, N., Thanmayi, V., Suchetha, M., Dhas, D. E., Sehastrajit, S., and Aakur, S. N. (2024). Pipelined structure in the classification of skin lesions based on AlexNet CNN and SVM model with bi-sectional texture features. *IEEE Access*, 12, 57366–57380.

[44] Vidhyalakshmi, A. M., and Kanchana, M. (2024). Classification of skin disease using a novel hybrid flash butterfly optimization from dermoscopic images. *Neural Computing and Applications*, 36(8), 4311–4324.

[45] Jaiyeoba, O., Ogbuju, E., Yomi, O. T., and Oladipo, F. (2024). Development of a model to classify skin disease using stacking ensemble machine learning techniques. *Journal of Computing Theories and Applications*, 2(1), 23–38.

[46] Rajeswari, R., Kalaiselvi, K., Jayshri, N., Lakshmi, P., and Muthusamy, A. (2024). Meta-heuristic-based melanoma skin disease detection and classification using Wolf Antlion Neural Network (WALNN). *International Journal of Intelligent Systems and Application in Engineering*, 12(9), 87–95.

[47] Ghaleb, S. A. M., and Bahmaid, S. (2025). Early skin disease detection using hybrid machine learning model for Vision 2030 of the Kingdom of Saudi Arabia. *International Journal of Intelligent Engineering and Systems*, 18(2), 64–75.

[48] Abdulredah, A. A., Fadhel, M. A., Alzubaidi, L., Duan, Y., Kherallah, M., and Charfi, F. (2025). Towards unbiased skin cancer classification using deep feature fusion. *BMC Medical Informatics and Decision Making*, 25(48), 2–22.

[50] Abbas, S., Ahmed, F., Khan, W. A., Ahmad, M., Khan, M. A., and Ghazal, T. M. (2025). Intelligent skin disease prediction system using transfer learning and explainable artificial intelligence. *Scientific Reports*, 15, 1–13.

[51] Ayoade, O. B., Raji, O. M., Akindele, A. A., Yusuf-Mashopa, K. J., Abdulrauff, M. F., Raji, I. A., and Musah, F. B. (2025). Non-hybrid machine learning techniques for classifying and detecting skin disease variants. ABUAD Journal of Engineering and Applied Sciences (AJEAS), 3(1), 145–159.

[52] Al-Himyari, B. A., Al-Khafaji, H., and Hussain, N. F. (2024). Exploration–exploitation trade-offs in metaheuristics: A review. Asian Journal of Applied Sciences, 12(1), 1–21. https://ajouronline.com/index.php/AJAS/article/view/7338/3893

[53] Sharma, H., Bharali, J., Motghare, M., Arora, K., Yoon, C., and Joshi, G. P. (2025). Development and evaluation of hybrid Harris Hawks optimization algorithms for advanced engineering applications. Scientific Reports, 15, 1–10. https://www.nature.com/articles/s41598-025-23624-5.pdf

[54] Wang, Z., and Wei, X. (2025). Harris Hawk optimization algorithm with combined perturbation strategy and its application. Scientific Reports, 15, 1–43. https://www.nature.com/articles/s41598-025-04705-x.pdf

[55] Yang, T., Fang, J., Jia, C., Liu, Z., and Liu, Y. (2023). An improved Harris Hawks optimization algorithm based on chaotic sequence and opposite elite learning mechanism. PLOS ONE, 18(2), 1–15. https://journals.plos.org/plosone/article/file?id=10.1371/journal.pone.0281636&type=printable

[56] Wang, S., Jia, H., Liu, Q., and Zheng, R. (2021). An improved hybrid Aquila optimiser and Harris Hawks optimisation for global optimisation. Mathematical Biosciences and Engineering, 18(6), 7076–7109.

[57] Makhmudova, D. M., and Almufti, S. M. (2024). Hybrid metaheuristic framework for multi-objective engineering optimization problems. Qubahan Techno Journal, 3(1), 1–14.

[58] Abdullahi, S., and Sathasivam, S. (2026). An enhanced hybrid framework for predictive analytics utilizing metaheuristic optimization techniques. Knowledge and Information Systems, 68(1), 1–10.

[59] Elhosseny, M., Abdel-Salam, M., and El-Hasnony, I. M. (2025). Adaptive dynamic crayfish algorithm with multi-enhanced strategy for global high-dimensional optimization and real-engineering problems. Scientific Reports, 15, 1–40. https://pmc.ncbi.nlm.nih.gov/articles/PMC11950391/pdf/41598_2024_Article_81144.pdf

[60] Tejani, G. G., Sharma, S. K., and Mishra, S. (2025). Parallel sub-class modified teaching learning-based optimization. Scientific Reports, 15, 1–38. https://www.nature.com/articles/s41598-025-10596-9.pdf

[61] Rizkallah, L. W. (2025). Optimizing SVM hyperparameters for satellite imagery classification using metaheuristic and statistical techniques. International Journal of Data

Science and Analytics, 20(5), 4945–4962. https://link.springer.com/content/pdf/10.1007/s41060-025-00762-7.pdf

[62] Ding, J., Du, J., Wang, H., and Xiao, S. (2025). A novel two-stage feature selection method based on random forest and improved genetic algorithm for enhancing classification in machine learning. Scientific Reports, 15, 1–16. https://www.nature.com/articles/s41598-025-01761-1.pdf

[63] Qi, K., Wei, K., Cheng, R., Liang, G., Hu, J., and Wu, W. (2025). An improved black-winged kite algorithm for global optimization and fault detection. Biomimetics, 10(11), 1–24. https://www.mdpi.com/2313-7673/10/11/728/pdf

[64] Alabed, T., and Servi, S. (2025). A Lévy flight-based chaotic black-winged kite algorithm for solving optimization problems. Scientific Reports, 15, 1–28. https://www.nature.com/articles/s41598-025-18196-3.pdf

[65] Guo, D., and Huang, H. (2025). Multi-strategy honey badger algorithm for global optimization. Biomimetics, 10(9), 1–30.

[66] Abualigah, L., Alomari, S. A., Almomani, M. H., Zitar, R. A., Migdady, H., Saleem, K., Smerat, A., Snasel, V., and Gandomi, A. H. (2025). Enhanced Aquila optimizer for global optimization and data clustering. Scientific Reports, 15, 1–36. https://www.nature.com/articles/s41598-025-95888-w.pdf

[67] Akl, D. T., Saafan, M. M., Haikal, A. Y., and El-Gendy, E. M. (2024). IHHO: An improved Harris Hawks optimization algorithm for solving engineering problems. Neural Computing and Applications, 36, 12185–12298. https://link.springer.com/content/pdf/10.1007/s00521-024-09603-3.pdf

[68] Wolpert, D. H., and Macready, W. G. (1997). No free lunch theorems for optimization. IEEE Transactions on Evolutionary Computation, 1(1), 67–82.

[69] Yang, X. S. (2012). Free lunch or no free lunch: That is not just a question? International Journal of Artificial Intelligence Tools, 21(3), 1–13.

[70] Uddin, S., and Lu, H. (2024). Dataset meta-level and statistical features affect machine learning performance. Scientific Reports, 14, 1–11. https://www.nature.com/articles/s41598-024-51825-x.pdf

[71] Dai, Q., Wang, L., Xu, K., Du, T., and Chen, L. (2024). Class overlap detection based on heterogeneous clustering ensemble for multi-class imbalance problems. Expert Systems with Applications, 255(1), 1–10.

[72] Mahmood, Z., Jamel, L., Salem, D. A., and Ashraf, I. (2025). Improving learning from complex multi-class imbalanced and overlapped data by mapping into higher dimensions

using SVM++. Scientific Reports, 15, 1–21. https://www.nature.com/articles/s41598-025-13929-w.pdf

[73] Shambour, Q., Al-Zyoud, M., and Almomani, O. (2025). Quantum-inspired hybrid metaheuristic feature selection with SHAP for optimized and explainable spam detection. Symmetry, 17(10), 1–34. https://www.mdpi.com/2073-8994/17/10/1716/pdf

[74] Ali, A. R., and Kamal, H. (2026). Hybrid HHO-WHO optimized transformer-GRU model for advanced failure prediction in industrial machinery and engines. Sensors, 26(2), 1–44.

[75] Makhmudova, D. M., and Almufti, S. M. (2024). Hybrid metaheuristic framework for multi-objective engineering optimization problems. Qubahan Techno Journal, 3(1), 1–14.

[76] Roeva, O., Zoteva, D., Roeva, G., Ignatova, M., and Lyubenova, V. (2024). An effective hybrid metaheuristic approach based on the genetic algorithm. Mathematics, 12(23), 1–15. https://www.mdpi.com/2227-7390/12/23/3815/pdf

[77] Ponzio, F., Urgese, G., Ficarra, E., and Di Cataldo, S. (2019). Dealing with lack of training data for convolutional neural networks: The case of digital pathology. Electronics, 8(3), 1–21. https://www.mdpi.com/2079-9292/8/3/256/pdf

[78] Alzubaidi, L., Bai, J., Al-Sabaawi, A., Santamaria, J., Albahri, A. S., Al-dabbagh, B. S. N., Fadhel, M. A., Manoufali, M., Zhang, J., Al-Timemy, A. H., Duan, Y., Abdullah, A., Farhan, L., Lu, Y., Gupta, A., Albu, F., Abbosh, A., and Gu, Y. (2023). A survey on deep learning tools dealing with data scarcity: Definitions, challenges, solutions, tips, and applications. Journal of Big Data, 10(46), 1–82. https://link.springer.com/content/pdf/10.1186/s40537-023-00727-2.pdf

[79] Gönen, M., and Alpaydın, E. (2011). Multiple kernel learning algorithms. Journal of Machine Learning Research, 12(64), 2211–2268. https://jmlr.csail.mit.edu/papers/volume12/gonen11a/gonen11a.pdf

[80] Islam, A., Bouzerdoum, A., and Belhaouari, S. B. (2024). Bio-inspired adaptive neurons for dynamic weighting in artificial neural networks. arXiv. https://arxiv.org/abs/2412.01454

[81] LeJeune, D., and Alemohammad, S. (2024). An adaptive tangent feature perspective of neural networks. In Proceedings of the Conference on Parsimony and Learning, Hong Kong, China (pp. 379–394).

[82] Abdulredah, A. A., Fadhel, M. A., Alzubaidi, L., Duan, Y., Kherallah, M., and Charfi, F. (2025). Towards unbiased skin cancer classification using deep feature fusion. BMC Medical Informatics and Decision Making, 25(48), 1–22.

[83] Hussain, S. I., and Toscano, E. (2025). Enhancing recognition and categorization of skin lesions with tailored deep convolutional networks and robust data augmentation techniques. Mathematics, 13(9), 1–36. https://www.mdpi.com/2227-7390/13/9/1480/pdf

[84] Zhang, Z. (2023). The transferability of transfer learning models based on ImageNet for medical image classification tasks. Applied and Computational Engineering, 18, 143–151.

[85] Ahmad, Z., Bao, S., and Chen, M. (2025). Performance evaluation of transfer learning-based medical image classification techniques for disease detection. arXiv. https://arxiv.org/abs/2512.04397